A study on CO_2 supersaturation in the Martian southern polar night using MGS radio occultation profiles rederived with MCS temperature climatology

K. Noguchi, *Faculty of Science, Nara Women's University, Nara, Japan (nogu@ics.nara-wu.ac.jp)*, **A. Kleinboehl, S. Piqueux**, *Jet Propulsion Laboratory, California Institute of Technology, Pasadena, USA*.

Introduction: Radio occultation (RO) measurements provide vertical profiles of temperature and pressure in a planetary atmosphere assuming that its atmospheric composition and a temperature at the uppermost altitude of each measurement are known. Fjeldbo and Eshleman [1] proposed the concept of RO for planetary explorations, and Fjeldbo and Eshleman [2] first conducted RO measurements in the Martian atmosphere utilizing the flyby of Mars by Mariner 4. Hinson et al. [3] retrieved vertical profiles of temperature and pressure from RO measurements conducted by the Mars Global Surveyor (MGS) mission. In their retrievals, the authors assumed the Martian atmospheric composition obtained by the Viking Landers [4] and several typical temperature values at the uppermost altitude. The influence of these two assumptions is especially large in the polar winter regions of Mars, where the temperature is extremely low and supersaturation and condensation of CO_2 frequently occur [5, 6]. The CO_2 condensation is significant in the Martian atmosphere [7], and the high vertical resolution of temperature in RO measurements can contribute to the science of the polar winter regions [8].

In the present study, we consider changes of the atmospheric composition as well as the high-altitude temperature constraint in the Martian polar night when retrieving MGS RO data. We follow the method previously established by Noguchi et al. [9], which resolves one of the two problems, the change in atmospheric composition. We newly utilize the zonal-mean temperature climatology obtained by the Mars Climate Sounder (MCS) [10] onboard Mars Reconnaissance Orbiter (MRO) in order to solve the other problem, the temperature assumption at the uppermost altitude [11]. This update of the vertical profiles of temperature and pressure obtained from MGS RO measurements provides new insights into the supersaturation of CO_2 in the southern polar winter region of Mars.

Data and Method: We utilized the MGS-RO data set [12] available from the NASA Planetary Data System (PDS). The original data set contains more than 20,000 vertical profiles, including atmospheric pressure, temperature, number density and their errors during four Martian years from Mars Year (MY) 24 to 27 (see Piqueux et al. [13] for a description of MY). Following the method proposed by Noguchi et al. [9, 11], we rederived 2,065 of the MGS- RO vertical profiles of temperature and pressure in the latitudes between 60°S–90°S during Ls=30°–220°, which corresponds to the southern polar night regions.

In the rederivation, we utilize the temperature data set obtained by MRO-MCS observations to replace the temperature assumed at the uppermost altitude (hereafter T^u). The MRO-MCS data set is available from the NASA Planetary Data System (PDS). The data set contains millions of vertical profiles including atmospheric pressure, temperature, extinctions of water ice clouds and dust and their errors from MY 28 to the present. Those physical quantities are retrieved from measurements of thermal emission in limb geometry, covering a vertical range from near the surface to 80-90 km altitude [14]. The data set is based on an improved algorithm that considers the two-dimensional structure of the atmosphere along the line of sight of the limb measurement [15]. This improves the accuracy of the retrieved quantities in regions that have strong horizontal gradients of temperature and aerosols, which is particularly important for the study of the winter polar regions, where strong gradients are encountered.

Because there is no overlapping time period between the MGS and MRO observations, we use data from different MYs of MRO mission in order to create a temperature climatology to serve as a replacement for T^u. The southern winter season is less influenced by dust and less interannually variable than the dusty season [16]. Therefore, we simply averaged the temperature profiles obtained by MRO-MCS in MY29–33 to create a zonal temperature climatology. We gridded the zonal averages into bins of five degrees in Ls and latitude.

The CO_2 saturation temperature (T_s) for a given pressure, is calculated by the formula shown in Kasting [17].

Results: The zonal averages of the difference between the rederived temperature and T_s are shown in the latitude–altitude cross section (Figure 1) and Ls–altitude cross sections (Figure 2), where negative values, which are shown in purple, indicate CO_2 supersaturation. The supersaturation mainly occurs south of 65°S and extends to an altitude of about 15 km. The temperature in the supersaturation regions is at most a few kelvins below T_s. After the winter solstice (Ls>90°), the vertical extent of the supersaturation decreases rapidly, yet remains several kilometers above the surface at high latitudes, as illustrated

in Figures 1(d) and (e). Even beyond the spring equinox (Ls>180°), a thin layer just above the surface continues to exhibit low temperatures, at least between latitudes of 70°S and 60°S, where it is not significantly supersaturated. The observed seasonal variations in the vertical structure of supersaturation and temperature align with the evolution of the southern seasonal polar caps [7, 13], which cover their largest surface area at the winter solstice and still extend to at least 60°S or further south by the spring equinox. This suggests that the polar caps, persisting after spring, continue to cool the air immediately above the surface.

To further examine the near-surface thermal structure, we analyzed vertical profiles of rederived temperature before and after the spring equinox (Ls=180°). Before the equinox, in the polar night, the temperature profiles at lower altitudes generally follow the CO_2 saturation curve. After the equinox, however, the profiles often exhibit strong temperature inversions extending up to about 5 km above the surface. These changes suggest that the boundary layer evolves markedly with season, influenced by surface-atmosphere interactions and thermal inertia after the seasonal polar cap begins to retreat.

Concluding Remarks: We have provided evidence for supersaturation with respect to CO_2 in the Martian southern polar night and examined its vertical structure and its dependence on latitude and Ls by using MGS RO measurements. We improved the retrievals of RO measurements by correcting the upper boundary temperature T^u, using the MRO MCS temperature measurements. The analysis of the updated MGS RO temperature vertical profiles shows that the supersaturation mainly occurs south of 65°S and extends to an altitude of about 15 km. After the winter solstice, the height of the supersaturation decreases rapidly but remains a few kilometers thick at high latitudes. Even after the spring equinox, a thin layer just above the surface still stays at a low temperature at least in the latitude range of 70°S–60°S. The temperature below T_s in the supersaturated regions is at most a few kelvins.

Acknowledgments: Initial work on this project was performed during a visit of K. N. to Jet Propulsion Laboratory (JPL), California Institute of Technology funded by the JPL Science Visitor Colloquium Program. The authors are grateful to David P. Hinson and the MGS radio occultation team for providing pressure-temperature data from the radio occultation measurements. The MGS radio occultation data are available at the Geosciences Node of the National Aeronautics and Space Administration (NASA) Planetary Data System (PDS). This work was partially supported by JSPS KAKENHI Grant Number 19K03951 and 22K03701. The MCS data are available at the Atmospheres Node of PDS. Work at JPL is performed under contract with NASA (80NM0018D0004).

References: [1] Fjeldbo, G., and Eshleman, V. R. (1965) *JGR, 70,* 3217–3225. [2] Fjeldbo, G., and Eshleman, V. R. (1968) *Planet. Space Sci., 16 (8)*, 1035–1059. [3] Hinson, D. P. et al. (1999) *JGR, 104 (E11),* 26997–27012. [4] Owen, T. et al. (1977) *JGR, 82 (28),* 4635–4639. [5] Kieffer, H. H. et al. (1977) *JGR 82 (28),* 4249–4291. [6] Hayne, P. O. et al. (2012) *JGR, 117,* E08014. [7] Haberle, R. M. (Eds.) (2017) *Cambridge University Press.* [8] Hu, R. et al. (2012) *JGR, 117,* E07002. [9] Noguchi, K. et al. (2014) *JGR, 119 (12),* 2510–2521. [10] McCleese, D. J. et al. (2007) *JGR, 112,* E05S06. [11] Noguchi, K. et al. (2022) *7th MAMO workshop,* abstract (poster). [12] Tyler, G. L. et al. (2001). *JGR, 106 (E10)*, 23327–23348. [13] Piqueux, S. et al. (2015) *Icarus, 251,* 164–180. [14] Kleinboehl, A. (2009) *JGR, 114,* E10006. [15] Kleinboehl, A. et al. (2017) *J. Quant. Spectr. Rad. Trans., 187,* 511–522. [16] Kass, D. M. et al. (2016) *GRL, 43 (12)*, 6111-6118. [17] Kasting, J. F. (1991) *Icarus, 94 (1),* 1–13.

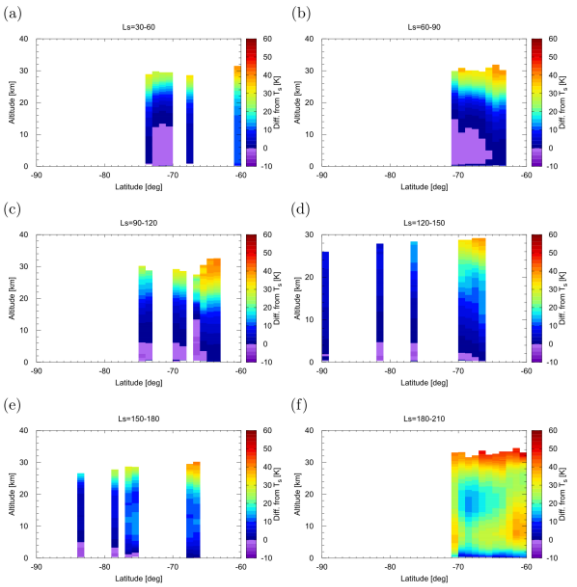

Figure 1: Latitude and altitude cross sections of zonal averages of the difference between rederived temperature and T_s in the Ls intervals of (a) 30°–60°, (b) 60°–90°, (c) 90°–120°, (d) 120°–150°, (e) 150°–180° and (f) 180°–210°.

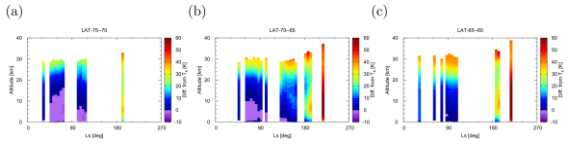

Figure 2: Same as Figure 1, but for Ls and altitude cross sections in the latitudes of (a) 75°S–70°S, (b) 70°S–65°S and (c) 65°S–60°S.